symmetry

MDPI

Article

Photon Acceleration by Superluminal Ionization Fronts

José Tito Mendonça

GoLP/IPFN, Instituto Superior Técnico, Universidade de Lisboa, Av. Rovisco Pais 1, 1049-001 Lisboa, Portugal; titomend@tecnico.ulisboa.pt

Abstract: This paper explores the use of superluminal ionization fronts to accelerate and amplify electromagnetic radiation. These fronts are defined as optical boundaries between two regions of a gas, the neutral region and the plasma region, characterized by two different values of the refractive index. For that reason, the front velocity is not necessarily related to the motion of material particles, such as neutral atoms, ions and electrons, which can stay at rest. The fronts can therefore become superluminal without violating causality. In recent years, different experimental configurations, such as the flying focus, showed that it is possible to create superluminal fronts in the laboratory. These fronts can easily be described theoretically in a special reference frame, called the time frame, which is used here. In this frame, superluminal fronts reduce to time refraction, a process that is symmetrical to the well-known optical refraction. It is shown that propagation through such fronts can lead to considerable frequency shifts and energy amplification of probe laser beams. This could eventually be used to develop new sources of tunable radiation.

Keywords: plasmas; ionization fronts; superluminal; photon acceleration; time refraction; lasers

1. Introduction

The interaction of light with ionization fronts is an old theoretical problem in plasma physics [1,2] and led to the foundations of the concept of photon acceleration [3–5]. This concept is intimately related to the effect of self-phase modulation that is studied in nonlinear optical media [6], as shown in [7]. One of the most spectacular manifestations of self-phase modulation is the supercontinuum laser source (see [8]). Another extension of the problem of propagation in ionization fronts is associated with the possible use of superluminal fronts. This leads to the exploration of interesting space–time symmetries, as discussed here.

The theory of superluminal fronts was first considered in terms of geometric optics, showing that very large values of frequency shifts could be attained [9]. It should be noticed that the velocity of an ionization front is not directly associated with any material motion because it is defined as an optical boundary between two regions of a gas, the neutral region and the ionized gas region, with two different refractive indices. As such, it can in principle be achieved with particles at rest (neutral atoms, electrons and ions) in the same way as a front fire can move in a forest with the trees staying at rest.

In the past, several experiments explored the use of relativistic ionization fronts moving with velocities close to, but lower than, the speed of light c [10–13]. Until recently, there was no clear indication that superluminal fronts, moving with velocities above c, could be generated experimentally. However, in recent years, the practical implementation of superluminal boundaries became possible due to the proposed schemes of *flying focus* [14–17] (see also [18]). They are mainly based on chromatic optics, but achromatic schemes can also in principle be conceived [19,20]. We could therefore use the flying focus, or some other equivalent concept, to propose a new type of radiation experiments based on superluminal fronts. It is the purpose of the present work to describe the basic radiation processes induced by such fronts and show the underlying symmetry-breaking processes that can take place in space and time boundaries.

check for updates

Citation: Mendonça, J.T. Photon Acceleration by Superluminal Ionization Fronts. *Symmetry* **2024**, *16*, 112. https://doi.org/10.3390/sym16010112

Academic Editor: Fabio Sattin

Received: 19 December 2023
Revised: 12 January 2024
Accepted: 15 January 2024
Published: 18 January 2024

The content of this paper is the following. In Section 2, superluminal fronts are described in the laboratory frame S and in the time frame S'. It is shown that this new frame S' moves with respect to the laboratory frame with a subluminal velocity $V < c$ and can therefore be characterized by a proper Lorentz transformation. The interest of this new frame is that the superluminal front is reduced to a purely temporal process, to which the model of time refraction can be directly applied [21,22]. Two front shapes are defined, a simple front with a constant electron density and a modulated front with electron density oscillations. Simple fronts can easily be created by short laser pulses because the recombination times are much longer than the ionization times, and the electron density stays nearly constant behind the pulse front [12]. The case of a modulated front is more speculative, although some recent simulations show that laser wakefields sometimes seem to behave as superluminal density waves, similar to the model examined here [23]. But this is only valid under quite special conditions, and the use of this approach to create superluminal density oscillations is questionable.

In Section 3, a simple front shape is considered, and the frequency shifts of a probe laser beam interacting with the front are derived. It is shown that they strongly depend on the direction of propagation of the probe beam with respect to the ionization front. In Section 4, the field transformation formulas are used to derive expressions for the reflection and transmission coefficients in both reference frames. They can be seen as temporal Fresnel's formulas. In Section 5, we consider the case of a modulated front and show that resonant scattering conditions characterized by a temporal Bragg formula can also be defined. If possible, the use of such modulated fronts with oscillating density perturbations behind the front could lead to the formation of a time crystal. Finally, in Section 6, we state some conclusions.

The present work is valid in the frame of classical radiation theory, but the quantum optical description could equally be possible [24–26]. We adapt our previous results of time refraction to the case of a time frame. Notice that time refraction is a general process, symmetric to the well-know optical refraction, that exists in the classical as well as in the quantum regime. Time refraction was recently extended to the case of a Dirac field [27,28], where photons are replaced by electron–positron pairs.

2. Time Frame

Let us consider the plasma-density perturbations associated with an ionization front, moving with superluminal velocity $u > c$, along some arbitrary x-direction. We first describe the front in the laboratory frame S and then introduce the *time frame* S', where the front will appear as a purely temporal process, enabling a simpler discussion of the wave propagation through the front.

The front can be generically described by the electron plasma frequency profile, $\omega_p(\mathbf{r}, t)$. We use the square of this frequency because it is proportional to the electron plasma density and it is a relativistic invariant. In the lab frame, a front moving with velocity u along a given x-axis can be described by the following expression:

$$\omega_p^2(x,t) = \omega_{p0}^2[1 + \epsilon g(x,t)] f(x,t) \,, \tag{1}$$

where $f(x,t)$ describes the shape of the front itself as it is created by a laser pulse that moves through the medium and $g(x,t)$ describes the eventual density structure with amplitude ϵ left behind the front. This structure can be a plasma-density oscillation moving with the front, as considered later. But, for the moment, we consider a flat front with no structure and assume the amplitude $\epsilon = 0$. For simplicity, we also ignore the transverse dimension, $\mathbf{r}_\perp$, which can easily be included if necessary. In our description, it is appropriate to use

$$f(x,t) = \frac{1}{2}\Big\{1 + tanh[k_f q(x,t)]\Big\} \,, \quad q(x,t) = x - ut \,. \tag{2}$$

where the quantity k_f defines the front width, and we assume a superluminal front velocity $u > c$. It is particularly useful to consider a Lorentz transformation from the lab frame S to a moving frame S', where the new front velocity becomes infinite, $u' \to \infty$. In this case, we are reduced to a purely temporal process where the plasma density instantly changes everywhere. To define this frame, we consider the new space and time variables (x', t'), defined by the Lorentz transformations:

$$x = \gamma(x' + Vt'), \quad t = \gamma\left(t' + \frac{\beta}{c}x'\right), \tag{3}$$

where V is the velocity of the new frame S' with respect to the lab, $\beta = V/c$ and $\gamma = (1-\beta^2)^{-1/2}$. Using the formula for the addition of velocities, we have a new front velocity u' determined by

$$u' = \frac{u - V}{1 - u\beta/c}, \tag{4}$$

which shows that u' diverges for $u = c/\beta \equiv c^2/V$. We conclude that this is a proper Lorentz transformation defined by a subluminal velocity $V = c^2/u < c$. Replacing this in the expression of $q(x,t)$, we obtain

$$q(x,t) = x - vt = \gamma\left(x' - \frac{c^2}{u}t'\right) - u\gamma\left(t' - \frac{x'}{u}\right) = \gamma(V - u)t'. \tag{5}$$

We conclude that the plasma frequency, given by Equations (1) and (2) with $\epsilon = 0$, only changes with time in the moving frame S'. We are therefore reduced to a purely temporal problem. For that reason, we will call S' the *time frame*. Noting that the plasma frequency is a relativistic invariant, we can conclude from this discussion that, in the new frame, the ionization front is given by

$$\omega_p^2(t') = \frac{\omega_{p0}^2}{2}\left[1 + tanh(\nu_f' t')\right], \tag{6}$$

with $\nu_f' = k_f\gamma(V - u)$. Please see Figure 1.

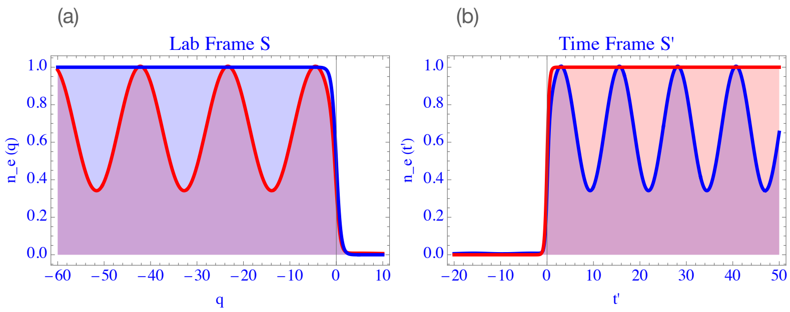

Figure 1. Superluminal ionization fronts, (**a**) in the laboratory frame S and (**b**) in the time frame S', for a simple front (in red) and a modulated front (in blue).

3. Frequency Shifts

Let us now assume a photon beam (for instance, a laser probe) interacting with the ionization front. Before interacting with the front, it will have an initial frequency ω_i defined in the lab frame. For propagation along the same x-axis, we can define the corresponding wavevector as $\mathbf{k}_i = k_i\mathbf{e}_x$, with $k_i = s\omega_i/c$, where $s = +1$ corresponds to copropagation and $s = -1$ to counterpropagation with respect to the front. Note that, in copropagation, the interacting photons are overtaken by the front.

In the time frame S', this initial beam will be characterized by new values of frequency ω'_i and wavevector $\mathbf{k}'_i = k'_i \mathbf{e}_x$ defined by

$$k'_i = \gamma\left(k_i - \frac{\beta}{c}\omega_i\right), \quad \omega'_i = \gamma(\omega_i - V k_i)\,. \tag{7}$$

This can be rewritten as

$$k'_i = \gamma(s - \beta)\frac{\omega_i}{c}, \quad \omega'_i = \gamma\omega_i(1 - s\beta)\,. \tag{8}$$

From here, we immediately conclude that

$$k'_i = s\frac{\omega'_i}{c}, \quad \omega_i'^2 = \omega_i^2 \frac{1 - s\beta}{1 + s\beta}\,. \tag{9}$$

It means that, for copropagation $(s = 1)$, we have $k'_i > 0$, and $\omega'_i \ll \omega_i$ is expected. In contrast, for counterpropagation $(s = -1)$, we have $k'_i < 0$, and $\omega'_i \gg \omega_i$.

Let us consider the interaction of this incident beam with the front. In the time frame S', the photons suffer a transformation process when they cross the temporal boundary at $t' = 0$. This is the process of time refraction, which is already well-understood [5,24]. We know that this process conserves momentum (in the time frame) and induces a frequency shift. To simplify the discussion, we assume that the front width is negligible, $1/\nu'_f \to 0$, but for a finite width, the final result would be the same. Assuming that the local dispersion relation is satisfied, for $t' > 0$, the wavevectors and frequencies of the transmitted and reflected signal are given by

$$\mathbf{k}'_r = -\mathbf{k}'_i\,, \quad \mathbf{k}'_t = \mathbf{k}'_i\,, \quad \omega'_r = \omega'_t = \sqrt{\omega_{po}^2 + k_t'^2 c^2} \neq \omega'_i\,. \tag{10}$$

Similarly, we can write

$$\omega'_t = \frac{|k'_t| c}{n'}, \quad n' = \sqrt{1 - \frac{\omega_{p0}^2}{\omega_t'^2}}\,, \tag{11}$$

where n' is the refractive index of the medium in the moving frame. Using Equation (9), we can write the new frequencies in terms of the initial frequency ω_i, defined in the lab frame, as

$$\omega_t'^2 = \omega_i^2 \frac{1 - s\beta}{1 + s\beta} + \omega_{p0}^2\,. \tag{12}$$

As a final step, we need to establish the value of the transmitted frequency in the lab frame, ω_t. We use the Lorentz formula

$$\omega_t = \gamma(\omega'_t - V k'_t) = \gamma\omega'_t(1 + s\beta n')\,. \tag{13}$$

From here, we obtain

$$\omega_t^2 = \omega_i^2 \frac{(1 + s\beta n')^2}{(1 + s\beta)^2} + \omega_{p0}^2\,. \tag{14}$$

A similar description can be made for the reflected beam, the only difference being the direction of propagation. The result is

$$\omega_r^2 = \omega_i^2 \frac{(1 - s\beta n')^2}{(1 - s\beta)^2} + \omega_{p0}^2\,. \tag{15}$$

It becomes clear that the reflected and transmitted beams have very distinct frequencies in the lab frame. Similarly, the corresponding wavevectors $\mathbf{k}_r$ and $\mathbf{k}_t$ will be quite different, in contrast with what happens in the time frame. This leads to the obvious conclusion that the superluminal front introduces a space and time symmetry breaking simultaneously, thereby changing the frequencies and momenta of the reflected and transmitted photons. This is illustrated in Figure 2 for an initial frequency slightly above cutoff, $\omega_i = \sqrt{2}\omega_{p0}$. It should be noticed that large values of β can easily be accessed experimentally because they correspond to weakly superluminal front velocities. This means that very large frequency shifts should be expected.

To complete the description in the lab frame S, we only need to relate n' with the refractive index valid in this frame, n. This can be conducted by again using the Lorentz relations. They allow us to write formulas similar to Equation (7) but with the refractive index included as

$$k'_t = \gamma(sn - \beta)\frac{\omega_t}{c}, \quad \omega'_t = \gamma\omega_t(1 - s\beta n). \tag{16}$$

Now, using the relation $k'_t c = s\omega'_t n'$, we easily obtain an expression for the refractive index in the moving frame as

$$n' = \frac{(n - s\beta)}{(1 - s\beta n)}, \quad n = \frac{(n' + s\beta)}{(1 + s\beta n')}, \tag{17}$$

Obviously, the refractive indices for the reflected and transmitted signals are different because they have different frequencies and the medium is dispersive, $n(\omega_r) \neq n(\omega_t)$. This contrasts with what happens in the time frame S', where we have $n'(\omega'_r) = n'(\omega'_t)$, because the frequencies are equal, although distinct from the initial frequency ω'_i.

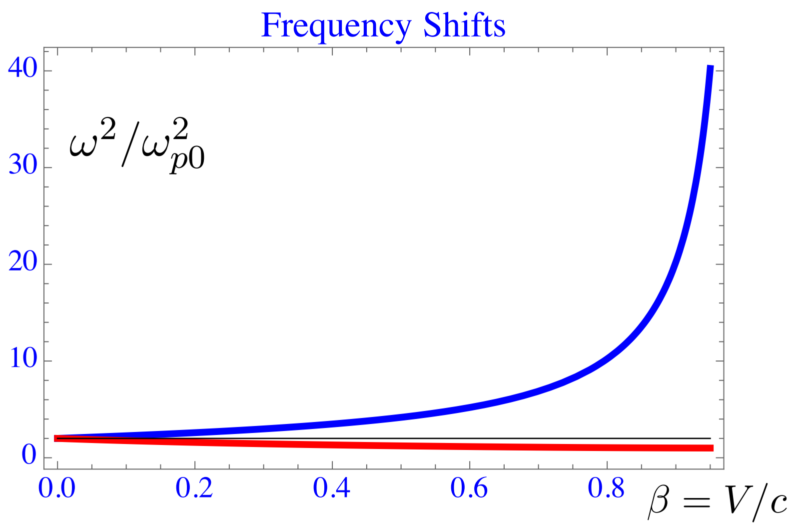

Figure 2. Frequency shifts for the transmitted and reflected beams, ω_t^2/ω_{p0}^2 (in blue) and ω_r^2/ω_{p0}^2 (in red), as a function of the frame velocity $\beta = V/c = c/u$ for an incident frequency $\omega_i = \sqrt{2}\omega_{p0}$.

4. Field Transformations

Let us now focus on the field transformations and establish the transmission and reflection coefficients in the two reference frames, S and S'. We start with the electric field $\mathbf{E}_i$, associated with the incident photon beam in the laboratory frame S. Assuming plane wave propagation along the x-axis, and neglecting the radial beam structure, we have

$$\mathbf{E}_i(x,t) = \mathbf{E}_i \exp(ik_i x - i\omega_i t), \tag{18}$$

with $k_i = s\omega_i/c$. Assuming that this field is linearly polarized in the y direction, $\mathbf{E}_i = E_i \mathbf{e}_y$, the wave magnetic field will be $\mathbf{B}_i = s(E_i/c)\mathbf{e}_z$. In the moving frame S', the field is described by a similar expression:

$$\mathbf{E}'_i(x,t) = \mathbf{E}'_i \exp(ik'_i x' - i\omega'_i t'), \tag{19}$$

where k'_i and ω'_i are determined by Equation (9). The field amplitudes will be determined by the Lorentz formulas as

$$\mathbf{E}'_i = \gamma(\mathbf{E}_i + \mathbf{V} \times \mathbf{B}_i) = \gamma(1 - s\beta)\mathbf{E}_i \,, \tag{20}$$

and

$$\mathbf{B}'_i = \gamma[\mathbf{B}_i - (\mathbf{V} \times \mathbf{E}_i)/c] = \gamma(1 - sV)\mathbf{B}_i \,, \tag{21}$$

In order to derive the fields resulting from the interaction with the ionization front, we use the reflection and transmission coefficients valid for a time refraction event as $E'_r = R'E'_i$ and $E'_t = T'E'_i$ such that [25]

$$T' = \frac{\alpha'}{2}(\alpha' + 1) \,, \quad R' = \frac{\alpha'}{2}(\alpha' - 1) \,, \tag{22}$$

where the parameter α' describes the change in the refractive index associated with the temporal transition from a vacuum with refractive index $n'_0 = 1$ to a plasma with refractive index n' as defined above. This is given by

$$\alpha' = \frac{n'_0}{n'} = \frac{(1 - s\beta n)}{(n - s\beta)} \,. \tag{23}$$

Noting that $\omega'^2_t = \omega'^2_i + \omega^2_{p0}$, we can also write

$$\alpha' = \frac{1}{n'} = \frac{\omega'_t}{\sqrt{\omega'^2_t - \omega^2_{p0}}} = \frac{\omega'_t}{\omega'_i} \,. \tag{24}$$

In previous papers on time refraction, these expressions for T' and R' were sometimes called temporal Fresnel's formulae. We can see that $T' + R' = \alpha'^2$, which is an indication that the energy is not conserved. See Figure 3 for an illustration. This could be explained at the elementary quantum level as the result of the emission of photon pairs from a vacuum [24,25]. Let us now use the expression for the transmitted field in the lab frame but now with the reversed sign of V in the transformation (21) and the inclusion of the refractive index. This gives

$$E_t = \gamma(1 + s\beta n')E'_t = TE_i \,, \quad E_r = \gamma(1 - s\beta n')E'_r = RE_i \,. \tag{25}$$

We then obtain the reflection and transmission coefficients in the lab frame as

$$T = \gamma^2(1 + s\beta n')(1 - s\beta)T' \,, \quad R = \gamma^2(1 - s\beta n')(1 - s\beta)R' \,, \tag{26}$$

and finally

$$T = \frac{(1 + s\beta n')}{(1 + s\beta)} \frac{1 + n'}{2n'^2} \,, \quad R = \frac{(1 - s\beta n')}{(1 + s\beta)} \frac{1 - n'}{2n'^2} \,, \tag{27}$$

where n' can be described in terms of the refractive index in the laboratory frame n by using Equation (17). In the absence of ionization, we would have $n = n' = 1$, and these expressions would reduce to $T = 1$, $R = 0$, as expected. But this result is not very illuminating because T and R are implicit functions of the transmitted and reflected frequencies. A more direct way to estimate the energy gain associated with this temporal process is to note that no dissipation is involved (apart from eventual scattering losses). Therefore, for each photon that crosses the time boundary, we have an energy gain that is exactly given by the frequency ratio ω_t/ω_i and ω_r/ω_i, where these quantities are determined by Equations (14) and (15).

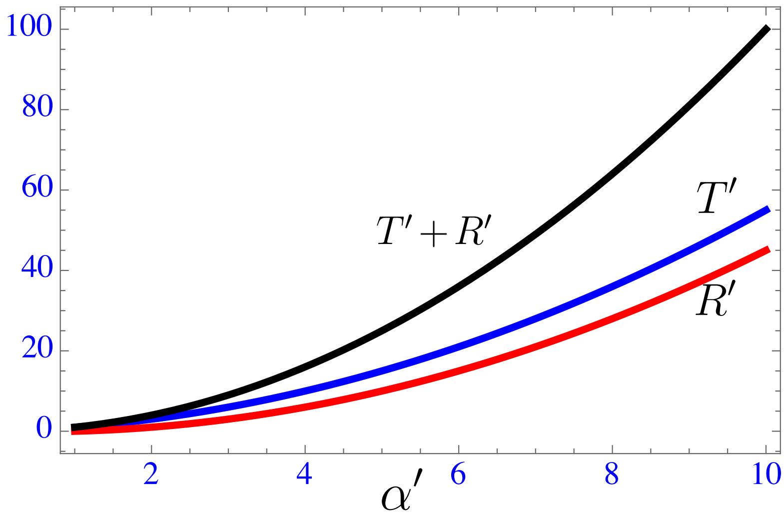

Figure 3. Transmission and reflection coefficients: in the moving frame, T' (in blue) and R' (in red), as a function of $\alpha' = \omega'_t/\omega'_i$. The quantity $T' + R'$ is also represented (in black).

5. Modulated Fronts

Let us now consider the case of modulated fronts, where the amplitude of the oscillations in Equation (1) is nonzero, $\epsilon \neq 0$, and the oscillating structure moves with the same superluminal speed as the front itself, $u > c$. For that purpose, we use a periodic function of the form

$$g(x,t) = \sum_\ell g_\ell \cos(\ell k_w q)\,, \tag{28}$$

where $q = x - ut$ as before; $g_\ell \leq 1$ are constant coefficients; and $k_w \ll k_f$ is the wavenumber of the periodic structure, defining a scale that is much larger than the front width. In the time frame S', the plasma frequency structure is now transformed into

$$\omega_p^2(t') = \frac{\omega_{p0}^2}{2}\left[1 + \epsilon \sum_\ell g_\ell \cos(\ell\omega'_w t')\right]\left[1 + tanh(\nu'_f t')\right], \tag{29}$$

with $\nu'_f = k_f\gamma(V-u)$, as before, and $\omega'_w = (k_w/k_f)\nu'_f$. Let us assume an incident wave with frequency ω_i, characterized by ω'_i and $\mathbf{k'}_i$ in the moving frame S', as defined by Equation (9). Assuming that the local dispersion relation is satisfied, after the transition time $t' = 0$, we have two wave modes with wavevectors $\mathbf{k'}_r = -\mathbf{k'}_i$ and $\mathbf{k'}_t = \mathbf{k'}_i$ and frequencies

$$\omega'_r = \omega'_t = \sqrt{\omega_p^2(t') + k_t'^2 c^2} \neq \omega'_i\,. \tag{30}$$

Here, the plasma frequency $\omega_p(t')$ is determined by Equation (29) and defines a time-varying dispersion relation. Notice that the wavenumbers remain fixed in this frame, but the frequencies are time-dependent. This means that we have to write the total field as

$$\mathbf{E'}_i(x',t') = \mathbf{E'}_t(t')\exp[(ik'_t x' - i\varphi(t')] + \mathbf{E'}_r(t')\exp[(ik'_r x' + i\varphi(t')] + c.c.\,, \tag{31}$$

with $\varphi(t') = \int^{t'} \omega'_{r,t}(t'')dt''$, valid for $\omega'_r = \omega'_t \neq \omega'_i$. This expression is valid for all times. From the field continuity relations, we can derive the following evolution equations for the field amplitudes [29]:

$$\frac{dE'_t}{dt'} = -\frac{1}{2}\frac{d\ln n'}{dt'}\left\{3E'_t + E'_r\exp[2i\varphi(t')]\right\}, \tag{32}$$

and

$$\frac{dE'_r}{dt'} = -\frac{1}{2}\frac{d\ln n'}{dt'}\left\{3E'_r + E'_t\exp[-2i\varphi(t')]\right\}, \tag{33}$$

where $n' \equiv n'(t') = \sqrt{1 - \omega_p^2(t')/\omega'^2}$ is the local refractive index. These expressions can be derived by using a succession of infinitesimal time-refraction processes. They can be used to describe propagation in arbitrary time-varying media and are formally identical to the field equations for propagation in static but arbitrarily inhomogeneous media [30,31]. Now, introducing the notation

$$E'_{r,t} = A'_{r,t} e^{-3\Gamma(t')} \,, \quad \Gamma(t') = \frac{1}{2} \int^{t'} \frac{d \ln n'}{dt''} dt'' \,, \tag{34}$$

we can reduce the above coupled equations for the amplitudes to the simple coupled form

$$\frac{dA'_t}{dt'} = \eta(t') A'_r \,, \quad \frac{dA'_r}{dt'} = \eta^*(t') A'_r \,, \tag{35}$$

with the new coefficient

$$\eta(t') = -\frac{1}{2} \left(\frac{d \ln n'}{dt'} \right) \exp\left[2i\varphi(t')\right] . \tag{36}$$

The solution of these equations is very easy to find and takes the form

$$A'_t(t') = \alpha(t') A'_t(0) - \beta(t') A'_r(0) \,, \quad A'_r(t') = \alpha(t') A'_r(0) - \beta(t') A'_t(0) \,, \tag{37}$$

where

$$\alpha(t') = \cosh\left[r(t')\right] , \quad \beta(t') = \sinh\left[r(t')\right] , \quad r(t') = \int^{t'} \eta(t'') dt'' . \tag{38}$$

The temporal evolution described by the coefficients $\alpha(t')$ and $\beta(t')$ can be seen as a squeezing transformation, where the quantity $r(t')$ is the squeezing parameter. Let us consider the initial conditions corresponding to the absence of a reflected field at the transition time $t' = 0$. Using $A'_t(0) \neq 0$ and $A'_r(0) = 0$ in Equation (37), we can then derive the time-reflection and time-transmission coefficients in the time frame S' as

$$T(t') = \frac{E'_t(t')}{E'_t(0)} = \cosh\left[r(t')\right] e^{-3\Gamma(t')} \,, \quad R(t') = \frac{E'_r(t')}{E'_t(0)} = \sinh\left[r(t')\right] e^{-3\Gamma(t')} \,, \tag{39}$$

These coefficients strongly depend on the amplitude of the moving structure, ϵ. Noting that $dn'/dt' \propto \epsilon$, we conclude that for very small modulation amplitudes, the following approximate solutions are valid:

$$T(t') \simeq 1 \,, \quad R(t') \simeq r(t') = -\frac{1}{2} \int^{t'} \left(\frac{d \ln n'}{dt''} \right) \exp[2i\varphi(t'')] dt'' \,, \tag{40}$$

On the other hand, we maximize the value of $|R(t')|$ when the quantity in the integrand of Equation (40) is nearly constant. For a cosine perturbation of the refractive index, such that in Equation (29) the constant coefficients are defined by the Kroeneker symbol, as $g_\ell = \delta_{\ell 1}$, this maximum reflection condition is approximately given by

$$\nu \omega'_w t' - 2\varphi(t') = 0 \,, \tag{41}$$

where ν is an integer. Noting that $\varphi(t') \simeq (\omega_i'^2 + \omega_{p0}^2)^{1/2} t'$, and using the explicit expression for ω'_w, we can rewrite this condition as

$$\nu \gamma k_w (V - u) = 2(\omega_i'^2 + \omega_{p0}^2)^{1/2} . \tag{42}$$

This approximate condition defines what could be called a *temporal Bragg law*. It characterizes the occurrence of resonant backscattering from a temporal periodic perturbation, or in other words, resonant backscattering from a time crystal. In order to relate this to the value of the incident frequency, as seen in the lab frame, we can use the Lorentz transformations (8) and write

$$\nu\gamma k_w(V-u) = 2\sqrt{\gamma^2\omega_i^2(1-s\beta)^2+\omega_{p0}^2}\,. \tag{43}$$

Finally, we obtain

$$\omega_i^2 = \frac{1}{4\beta^2}\frac{(1-\beta)^2}{(1-s\beta)^2}\left[\nu^2k_w^2c^2+\omega_{p0}^2\beta^2(1+\beta)\right]. \tag{44}$$

For incident frequencies ω_i satisfying this relation, we should be able to observe the formation of a Bragg maximum of the backscattered signal from a plasma time crystal. On the other hand, for a very long time structure, we see from Equation (39) that the energy of the time-reflected signal can grow exponentially due to the sine hyperbolic function $\sinh[r(t')]$. Furthermore, due to the need for momentum conservation, the transmitted signal will necessarily grow as well, thus showing the formation of a temporal-driven instability. This is nothing but a classical analog of the dynamical Casimir effect. We should, however, notice that the above temporal Bragg scattering and the associated instability can only be observed with a modulated ionization front with a shape defined by Equation (29), which is not easy to produce experimentally.

6. Conclusions

Wave propagation in the presence of superluminal ionization fronts was studied. These fronts can be used to produce a considerable frequency shift and to amplify radiation. Two kinds of ionization fronts, simple fronts and modulated fronts, were discussed. A simple theoretical description was used, based on the time frame, where the fronts reduce to a purely temporal process.

The results of this paper could eventually inspire the development of new radiation sources, where phase coherence is conserved and frequency tuning could be achieved for different values of the front velocity. This process is, in principle, one hundred percent efficient, because all photons are equally phase-shifted. Energy amplification can also be achieved, because part of the front energy can be converted into radiation.

The present work can be expanded in several different directions, including a systematic numerical study of the spectral energy density and an estimate of losses due to scattering in the transverse beam direction. It could also be applied to the optics of metamaterials, where the study of temporal processes is becoming particularly relevant [32–35].

Funding: This research received no external funding.

Data Availability Statement: The data presented in this study are included in the Figures.

Acknowledgments: The author would like to thank Jorge Vieira and John Palastro for the stimulating discussions on the radiation processes associated with laser wakefields and ionization fronts.

Conflicts of Interest: The author declares no conflicts of interest.

References

1. Semenova, V.I. Reflection of Electromagnetic Waves from an Ionization Front. *Radiophys. Quantum Electron.* **1967**, *10*, 599–604. [CrossRef]
2. Lampe, M.; Ott, E.; J.H. Walker, J.H. Interaction of Electromagnetic Waves with a Moving Ionization Front. *Phys. Fluids* **1978**, *21*, 42.
3. Mendonça, J.T. Nonlinear Interaction of Wavepackets. *J. Plasma Phys.* **1979**, *22*, 15. [CrossRef]
4. Wilks, S.C.; Dawson, J.M.; Mori, W.B.; Katsouleas, T.; Jones, M.E. Photon Accelerator. *Phys. Rev. Lett.* **1989**, *62*, 2600. [CrossRef] [PubMed]
5. Mendonça, J.T. *Theory of Photon Acceleration*; Institute of Physics Publishing: Bristol, UK, 2001.
6. Boyd, R.W. *Nonlinear Optics*; Academic Press: San Diego, CA, USA, 1992.
7. Silva L.O.; Mendonça, J.T. Photon Kinetic Theory of Self-Phase Modulation. *Opt. Commun.* **2001**, *196*, 285. [CrossRef]
8. Alfano, R.R. (Ed.) *Ths Supercontinuum Laser Source*, 4th ed.; Springer Nature: Cham, Switzerland, 2022.

9. Silva L.O.; Mendonça, J.T. Photon Acceleration in Superluminous and Accelerated Ionization Fronts. *IEEE Trans. Plasma Sci.* **1996**, *24*, 316.
10. Savage, R.L., Jr.; Joshi, C.; Mori, W.B. Frequency Upconversion of Electromagnetic Radiation upon Transmission into an Ionization Front. *Phys. Rev. Lett.* **1992**, *68*, 946. [CrossRef]
11. Dias, J.M.; Stenz, C.; Lopes, N.; Badiche, X.; Blasco, F.; Santos, A.D.; Silva, L.O.e.; Mysyrowicz, A.; Antonetti, A.; Mendonça, J.T. Experimental Evidence of Photon Acceleration of Ultrashort Laser Pulses in Relativistic Ionization Fronts. *Phys. Rev. Lett.* **1997**, *78*, 4773.
12. Dias, J.M.; Lopes, N.C.; Silva, L.O.; Figueira, G.; Mendonça, J.T.; Stenz, C.; Blasco, F.; Santos, A.D.; Mysyrowicz, A. Photon Acceleration of Ultrashort Laser Pulses by Relativistic Ionization Fronts. *Phys. Rev. E* **2002**, *66*, 056406. [CrossRef]
13. Lopes, N.C.; Figueira, G.; Dias, J.M.; Silva, L.O.; Mendonça, J.T.; Balcou, P.; Rey, G.; Stenz, C. Laser Pulse Frequency Up-shifts by Relativistic Ionization Fronts. *EuroPhys. Lett.* **2004**, *66*, 371.
14. Sainte-Marie, A.; Gobert, O.; Quéré, F. Controlling the Velocity of Ultrashort Light Pulses in Vacuum through Spatio-temporal Couplings. *Optica* **2017**, *4*, 1298. [CrossRef]
15. Froula, D.H.; Turnbull, D.; Davies, A.S.; Kessler, T.J.; Haberberger, D.; Palastro, J.P.; Bahk, S.; Begishev, I.A.; Boni, R.; Bucht, S.; et al. Spatiotemporal Control of Laser Intensity. *Nat. Photon.* **2018**, *12*, 262.
16. Franke, P.; Turnbull, D.; Katz, J.; Palastro, J.P.; Begishev, I.A.; Bromage, J.; Shaw, J.L.; Boni, R.; Froula, D.H. Measurement and Control of Large Diameter Ionization Waves of Arbitrary Velocity. *Opt. Express* **2019**, *27*, 31978. [PubMed]
17. Li, Z.; Liu, Y.; Leng, Y.; Li, R. Investigating Group-Velocity-Tunable Propagation-Invariant Optical Wave-Packets. *Sci. Rep.* **2022**, *12*, 16102. [CrossRef] [PubMed]
18. Agarwal, K.; Bhatt, R.N.; Sondhi, S.L. Fast Preparation of Critical Ground States using Superluminal Fronts. *Phys. Rev. Lett.* **2018**, *120*, 210604. [CrossRef]
19. Kondakci, H. E.; Abouraddy, A.F. Optical Space-time Wave Packets of Arbitrary Group Velocity in Free Space. *Nat. Commun.* **2019**, *10*, 929. [CrossRef] [PubMed]
20. Yessenov, M.; , Free, J.; Chen, Z.; Johnson, E.G.; Lavery, M.P.L.; Alonso, M.A.; Abouraddy, A.F. Space-time Wave Packets Localized in All Dimensions. *Nat. Commun.* **2022**, *13*, 4573.
21. Mendonça, J.T.; Shukla, P.K. Time Refraction and Time Reflection: Two Basic Concepts. *Phys. Scr.* **2002**, *65*, 160. [CrossRef]
22. Plansinis, B.W.; Donaldson, W.R.; Agrawal, G.P. What is the Temporal Analog of Reflection and Refraction of Optical Beams. *Phys. Rev. Lett.* **2015**, *115*, 183901. [CrossRef]
23. Malaca, B.; Pardal, M.; Ramsey, D.; Pierce, J.R.; Weichman, K.; Andriyash, I.A.; Mori, W.B.; Palastro, J.P.; Fonseca, R.A.; Vieira, J. Coherence and Superradiance from a Plasma-Based Quasiparticle Accelerator. *Nat. Photon.* **2023**, *18*, 39–45. [CrossRef]
24. Mendonça, J.T.; Guerreiro, A.; Martins, A.M. Quantum Theory of Time Refraction. *Phys. Rev. A* **2000**, *62*, 033805. [CrossRef]
25. Mendonça, J.T.; Martins, A.M.; Guerreiro, A. Temporal Beam Splitter and Temporal Interference. *Phys. Rev. A* **2003**, *68*, 043801. [CrossRef]
26. Mendonça, J.T. *The Quantum Nature of Light*; Institute of Physics Publishing: Bristol, UK, 2022.
27. Mendonça, J.T. Temporal Klein Model for Particle-Pair Creation. *Symmetry* **2021**, *13*, 1361. [CrossRef]
28. Mendonça, J.T. Particle-pair Creation by High-harmonic Laser Fields. *Phys. Src.* **2023**, *98*, 125606.
29. Mendonça, J.T.; Guerreiro, A. Time Refraction and the Quantum Properties of Vacuum. *Phys. Rev. A* **2005**, *72*, 063805. [CrossRef]
30. Ginzburg, V.L. *Propagation of Electromagnetic Waves in Plasmas*; Gordon and Breach: New York, NY, YSA, 1961.
31. Kline, M.; Kay, I.W. *Electromagnetic Theory and Geometric Optics*; John Wiley & Sons: New York, NY, USA, 1965.
32. Shcherbakov, M.R.; Lemasters, R.; Fan, Z.; Song, J.; Lian, T.; Harutyunyan, H.; Shvets, G. Time-Variant Metasurfaces Enable Tunable Spectral Bands of Negative Extinction. *Optica* **2019**, *6*, 1441. [CrossRef]
33. Liu, C.; Alam, M.Z.; Pang, K.; Manukyan, K.; Reshef, O.; Zhou, Y.; Choudhary, S.; Patrow, J.; Pennathurs, A.; Song, H.; et al. Photon Acceleration Using a Time-Varying Epsilon-Near-Zero Metasurface. *ACS Photonics* **2021**, *8*, 716.
34. Yuan, L.; Fan, S. Temporal Modulation Brings Metamaterials into New Era. *Light Sci. Appl.* **2022**, *11*, 173.
35. Castaldi, G.; Rizza, C.; Engheta, N.; Galdi, V. Multiple Actions of Time-resolved Short-pulsed Metamaterials. *Appl. Phys. Lett.* **2023**, *122*, 021701. [CrossRef]